Available online at www.sciencedirect.com
SCIENCE DIRECT
Talanta 67 (2005) 947–954
Talanta
www.elsevier.com/locate/talanta

A study of intramolecular H-complexes of novel bis(heptamethine cyanine) dyes

Jun Seok Kim, Ravikumar Kodagahally, Lucjan Strekowski *, Gabor Patonay *

Department of Chemistry, University Plaza, Georgia State University, Atlanta, GA 30303, USA

Received 14 January 2005; received in revised form 11 April 2005; accepted 11 April 2005
Available online 12 May 2005

Abstract

Near-infrared (NIR) bis(heptamethine cyanine) (BHmC) dyes containing a flexible polymethylene linker between the two cyanine subunits are a novel class of compounds with versatile spectroscopic properties. The first bis-cyanine of this type is BHmC-10 (with a decamethylene bridge) that has been reported by us recently [G. Patonay, J.S. Kim, R. Kodagahally, L. Strekowski, Appl. Spectrosc., in press]. As part of this work, additional bis-cyanines BHmC-4, BHmC-6, and BHmC-8 were synthesized and their spectral properties were evaluated for the dyes free in solution and in the presence of human serum albumin (HSA). These bis-cyanines undergo H-type aggregation, mainly H-type intramolecular complexation between the two cyanine subunits, when free in aqueous solution. This H-type interaction in phosphate buffer (pH 7.2) is characterized by hypsochromic (H) absorption at 700 nm, low extinction coefficient, and low fluorescence quantum yield. By contrast, an analogous monomeric cyanine exhibits strong fluorescence under similar conditions. Upon binding with HSA, the fluorescence of BHmC-6 changes negligibly, that for BHmC-8 shows a slight increase, and the fluorescence of BHmC-4 is greatly increased. It is suggested that BHmC-4 binds with HSA in the open form exclusively, while the H-type intramolecular interaction in BHmC-6 is mostly retained in the complex with HSA. Bis-cyanine BHmC-4 may be of significant bioanalytical utility due to its negligible fluorescence in aqueous solution and a strong increase in fluorescence upon binding with a protein.

Keywords: Bis-heptamethine cyanine dye (BHmC); Human serum albumin (HSA); H-aggregates

1. Introduction

Near infrared fluorescence dyes have attracted considerable attention in bioanalyses. Reported analytical applications for near-infrared (NIR) dyes include enzymatic assays [1], hydrophobicity [2], metal ion and pH studies [3], immunoassays [4], drug displacement [5], and DNA sequencing applications [6].

When compared to their visible counterparts, NIR cyanine dyes have considerable advantageous photophysical properties [7–9]. First, in the UV–visible region of the electromagnetic spectrum the autofluorescence from biomolecules can be significant while very few biomolecules possess intrinsic fluorescence in the NIR region (670–1100 nm). Second, the aggregation phenomenon of NIR cyanine dyes in aqueous buffers can be utilized for studying complex biomolecules [10–13]. The aggregation (Fig. 1) results in the formation of different structures depending on the angle of slippage α and is usually described as H-aggregation (hypsochromic) and J-aggregation (bathochromic). H-aggregates are referred to as "card-pack" arrangement, whereas J-aggregates are known as "brickwork" arrangement. Large molecular slippage ($\alpha < \sim 32^\circ$) results in a bathochromic shift while small slippage ($\alpha > \sim 32^\circ$) results in a hypsochromic shift [12–14]. The type of aggregates is dependent on several factors such as dye structure, dye concentration, solvent polarity, pH, ionic strength, and temperature [15]. The interaction with biomolecules can enhance the low fluorescence quantum yield of H-aggregates [14] while it can quench the more fluorescent J-aggregates [16,17]. The quantum yields of H- and J-aggregates typically increase and

* Corresponding authors. Tel.: +1 404 651 3856; fax: +1 404 651 1416.
E-mail address: cheggp@panther.gsu.edu (G. Patonay).

0039-9140/$ – see front matter © 2005 Elsevier B.V. All rights reserved.
doi:10.1016/j.talanta.2005.04.025

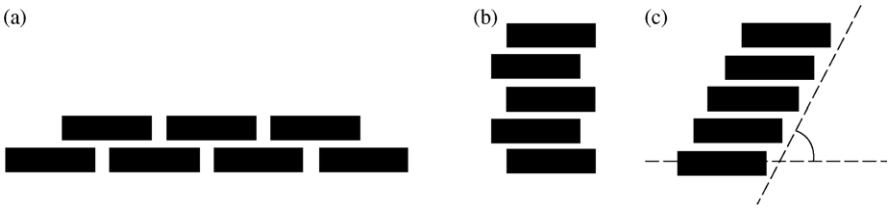

Fig. 1. Representative models of cyanine dye aggregates in solution: dye aggregates with brickwork (a); ladder (b); and staircase (c) molecular arrays; α is the angle of slippage. Aggregate models drawn after [13].

decrease, respectively, upon binding with proteins or other biomolecules. Fluorescence enhancement can be utilized for non-covalent labeling of the biomolecules [6,14]. Unfortunately, the monomeric cyanine dyes currently in use for non-covalent labeling purposes exhibit spectral properties that are strongly concentration-dependent. Concentration dependence is a major drawback in any bioanalytical application.

This concentration dependence is significantly reduced with a bis(heptamethine cyanine) dye BHmC-10 ($n = 10$ in Scheme 1), which has been evaluated in our previous work [14]. The designation BHmC-10 refers to a bis(heptamethine cyanine) with a 10-methylene (decamethylene) linker between the two cyanine subunits. BHmC-10 exhibits intramolecular and intermolecular van der Waals interaction that promotes H-aggregation, resulting in negligible fluorescence emission. Upon the addition of human serum albumin (HSA), the inter- and intramolecular complexes of BHmC-10 dissociate with concomitant increase in fluorescence, indicating a strong non-covalent interaction in the dye–HSA complex. The BHmC-10 dye–HSA interaction seems to readily promote opening up of the clam-shell form of the dimeric dye. As part of this work, new BHmCs with tetra-, hexa-, and octamethylene bridges were synthesized (Scheme 1), and their spectral properties were evaluated in the absence and presence of HSA. The results were compared to those of our previous studies with BHmC-10 and their monomeric counterpart.

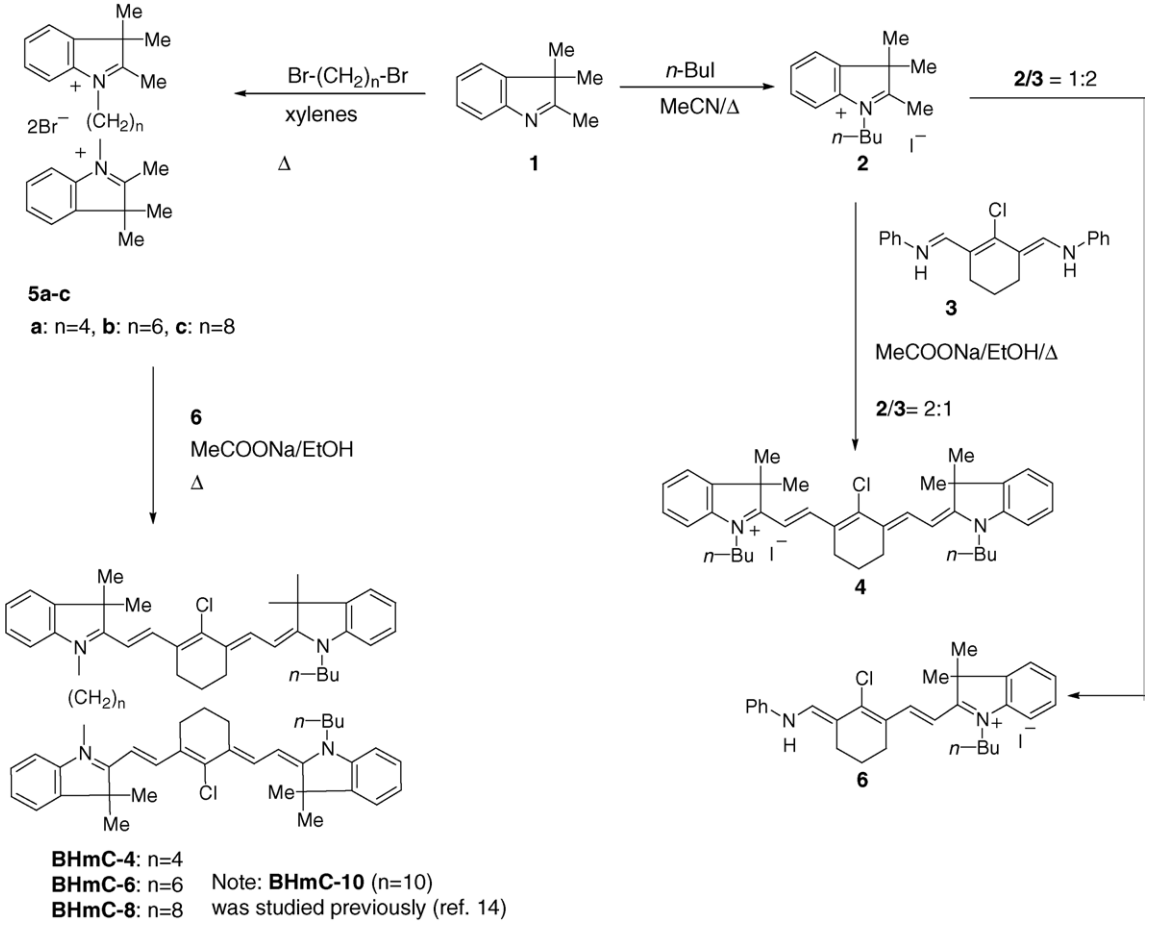

Scheme 1.

The aim was to better understand the spectral properties of a series of BHmCs containing polymethylene linkers of various lengths. Our results indicate that the length and rigidity of linkers strongly affect how strongly the carbocyanine moieties interact as well as the mode of intramolecular interactions in BHmCs. All these factors, in turn, have important ramifications for the interaction of bis-cyanines with HSA and their analytical utility.

2. Experimental

2.1. Synthesis of cyanine dyes

The preparation of the reference monomeric dye **4** (Scheme 1) has been described previously [14]. Briefly, indolenine **1** was quaternized by the reaction with butyl iodide followed by treatment of the resultant indolium derivative **2** with 0.5 equiv. of Vilsmeier-Haack reagent **3** [18]. On the other hand, the treatment of **2** with an excess of **3** gave a half-dye **6** as a major product [14]. In the synthesis of the desired bis-cyanines (BHmCs), indolenine **1** was quaternized by the reaction with an α,ω-dibromoalkane and then the resultant bis-indolium salt **5** was condensed with the reagent **6**. A general procedure for the synthesis and purification of BHmCs is given below.

A solution of **2** (0.34 g, 1 mmol), **3** (0.36 g, 1.5 mmol), and anhydrous sodium acetate (0.17 g, 2 mmol) in anhydrous ethanol (25 mL) was heated to 50 °C for 2 h under a nitrogen atmosphere. After concentration under reduced pressure the resultant mixture of **4** and **6** was separated by chromatography on silica gel eluting with ethyl acetate/hexanes (1:4). In a separate experiment, a mixture of **1** (0.48 g, 3 mmol) and an α,ω-dibromoalkane (1.5 mmol) was heated to 140 °C under a nitrogen atmosphere for 4 h. The resultant solid was extracted with acetone (3 × 10 mL). The extract was filtered and concentrated to give a solid residue of **5**. Product **5** was crystallized from methanol/ether.

The dimeric dyes were synthesized by heating under reflux for 24 h under a nitrogen atmosphere a solution of **6** (0.29 g, 0.5 mmol), **5** (0.25 mmol), and anhydrous sodium acetate (0.08 g, 1 mmol) in anhydrous ethanol (20 mL). After standard workup, BHmCs were isolated by silica gel chromatography eluting with ethyl acetate/dichloromethane (1:4). Two chromatographic separations were required to obtain the bis-cyanines in an analytically pure form.

The characterization of the intermediate products **5** and BHmCs is given below. The electron impact-induced mass spectra for **5** correspond to bis-anhydrobases (*M*–2HBr) that result from elimination of hydrogen bromide from **5** upon heating in the mass spectrometer. This is a general phenomenon for this class of compounds, including indolium salt **2**. Due to different *N*-substitution of the two cyanine subunits in BHmCs, their ^{1}H NMR spectra given below are complex. In particular, the signals for the pairs of methine protons H1′/H7′ (δ 6.22–6.37) and H2′/H6′ (δ 8.20–8.31) of the heptamethine moiety appear as two doublets for each pair.

Tetramethylene[bis(2,3,3-trimethyl-3H-indol-1-ium)] dibromide (**5a**): yield 60%; mp 103–104 °C; ^{1}H NMR (DMSO-d_6, 60 °C) δ 1.55 (s, 12H), 2.04 (m, 4H), 2.88 (s, 6H), 4.51 (m, 4H), 7.64 (m, 4H), 7.85 (m, 2H), 8.02 (m, 2H); EI MS *m*/*z* 372 $(M–2HBr)^+$.

Hexamethylene[bis(2,3,3-trimethyl-3H-indol-1-ium)] dibromide (**5b**): yield 67%; mp 110–111 °C; ^{1}H NMR (DMSO-d_6, 60 °C) δ 1.50 (m, 4H), 1.55 (s, 12H), 1.85 (m, 4H), 2.86 (s, 6H), 4.47 (m, 4H), 7.64 (m, 4H), 7.85 (m, 2H), 7.99 (m, 2H); EI MS *m*/*z* 400 $(M–2HBr)^+$.

Octamethylene[bis(2,3,3-trimethyl-3H-indol-1-ium)] dibromide (**5c**): yield 54%; mp 225–227 °C; ^{1}H NMR ($CDCl_3$, 28 °C) δ 1.57 (m, 4H), 1.67 (s, 12H), 2.07 (m, 4H), 2.67 (m, 4H), 3.31 (s, 6H), 4.86 (m, 4H), 7.59 (m, 4H), 7.63 (m, 2H), 7.83 (d, J = 7.5 Hz, 2H); EI MS *m*/*z* 428 $(M–2HBr)^+$.

Tetramethylene[bis[2-[7′-(1″-butyl-3″,3″-dimethylindolin-2″-ylidene)-4′-chloro-3′,5′-trimethylene-1′,3′,5′-heptatrien-1′-yl]-3,3-dimethyl-3H-indol-1-ium]] diiodide (**BHmC-4**): yield 17%; ^{1}H NMR (DMSO-d_6, 60 °C) δ 0.99 (t, J = 7 Hz, 6H), 1.10–2.00 (m + 3 s at δ 1.64, 1.71 and 1.72; 40H), 2.50–2.90 (m, 8H), 4.92 (m, 8H), 6.28 and 6.37 (2d, J = 14 Hz for each d, 4H), 7.20–8.00 (m, 16H), 8.21 and 8.31 (2d, J = 14 Hz for each d, 4H); MALDI MS *m*/*z* 1076.6 (M^+ for 2^{35}Cl), 1078.6 (M^+ for ^{35}Cl and ^{37}Cl), 1080.6 (M^+ for 2^{37}Cl). Analysis: Calcd. for $C_{72}H_{86}Cl_2I_2N_4$: C, 64.91; H, 6.51; N, 4.21. Found: C, 65.04; H, 6.61; N, 4.25.

Hexamethylene[bis[2-[7′-(1″-butyl-3″,3″-dimethylindolin-2″-ylidene)-4′-chloro-3′,5′-trimethylene-1′,3′,5′-heptatrien-1′-yl]-3,3-dimethyl-3H-indol-1-ium]] diiodide (**BHmC-6**): yield 17%; ^{1}H NMR (DMSO-d_6, 60 °C) δ 0.91 (t, J = 7 Hz, 6H), 1.10–1.90 (m + s at δ 1.63, 44H), 2.64 (m, 8H), 4.15 (m, 8H), 6.22 and 6.28 (2d, J = 14 Hz for each d, 4H), 7.25 (m, 4H), 7.36 (m, 8H), 7.56 (m, 4H), 8.20 and 8.25 (2d, J = 14 Hz for each d, 4H); MALDI MS *m*/*z* 1104.8 (M^+ for 2^{35}Cl), 1106.8 (M^+ for ^{35}Cl and ^{37}Cl), 1108.8 (M^+ for 2^{37}Cl). Analysis: Calcd. for $C_{74}H_{90}Cl_2I_2N_4{\cdot}2H_2O$: C, 63.65; H, 6.78; N, 4.01. Found: C, 63.61; H, 6.55; N, 4.29.

Octamethylene[bis[2-[7′-(1″-butyl-3″,3″-dimethylindolin-2″-ylidene)-4′-chloro-3′,5′-trimethylene-1′,3′,5′-heptatrien-1′-yl]-3,3-dimethyl-3H-indol-1-ium]] diiodide (**BHmC-8**): yield 17%; ^{1}H NMR (DMSO-d_6, 60 °C) δ 0.95 (t, J = 7 Hz, 6H), 1.09 (m, 4H), 1.20–1.90 (m + s at δ 1.66, 44H), 2.68 (m, 8H), 4.19 (m, 8H), 6.26 and 6.30 (2d, J = 14 Hz for each d, 4H), 7.29 (m, 4H), 7.41 (m, 8H), 7.60 (m, 4H), 8.25 and 8.27 (2d, J = 14 Hz for each d, 4H); MALDI MS *m*/*z* 1132.8 (M^+ for 2^{35}Cl), 1134.8 (M^+ for ^{35}Cl and ^{37}Cl), 1136.8 (M^+ for 2^{37}Cl). Analysis: Calcd. for $C_{76}H_{94}Cl_2I_2N_4{\cdot}4H_2O$: C, 62.50; H, 7.04; N, 3.84. Found: C, 62.48; H, 6.71; N, 4.20.

2.2. Other materials and solvents

Fatty acid free HSA (≥96% purity) was obtained from Sigma (St. Louis, MO). Sodium phosphate monobasic (monohydrate) and sodium phosphate dibasic (monohydrate) were purchased from Fisher Scientific (Fair Lawn, NJ).

Water was Nanopure grade (Barnstead model D4751 ultrapure water system). Methanol was obtained from the Aldrich Chemical Company (Milwaukee, WI) in HPLC grade.

2.3. Instrumentation

Absorption measurements were acquired on a Perkin-Elmer Lambda UV/VIS/NIR (Lambda 50) spectrophotometer (Norwalk, CT). Fluorescence emission spectra were taken using a K2 spectrofluorometer (ISS, Champaign, IL) equipped with a R928 Hamamatsu photomultiplier tube (Bridgewater, NJ). Commercial GaAlAs laser diodes (Laser Max, Rochester, NY) were used as the excitation source at 690 nm. The slit widths were 2 mm and the integration time was 3 s. All absorption and fluorescence measurements were taken in a 1 cm cuvette.

2.4. Methods

Stock solutions of the monomeric dye **4** (2 mM) and BHMCs (1 mM) in methanol were stored in the dark at 4 °C. The 0.1 mM stock solution of HSA was prepared in 20 mM dibasic phosphate buffer solution and adjusted to pH 7.2 with phosphoric acid. Stock solution of HSA was prepared fresh daily.

The dye–HSA mixture was vortexed for 30 s to allow for equilibration. Various dye–HSA ratios were investigated to determine the utility of BHmCs as non-covalent labels for serum albumins. For all experiments, the stock solution of BHmCs in methanol was diluted with phosphate buffer due to the relatively poor solubility of the dyes in aqueous solution. All working solutions contained only 1% (v/v) methanol to facilitate dye dissolution but to avoid denaturation of HSA. All measurements were performed at room temperature.

3. Results and discussion

3.1. Photophysical properties of BHmCs

3.1.1. BHmCs in methanol

Photophysical properties of these novel dimeric dyes in methanol were characterized. Spectral data obtained at the same concentrations (10 μM) of **4**, BHmC-4, -6, and -8, were normalized for direct comparison. The molar absorptivities (ε) of these dyes were determined using multiple concentrations, and no significant spectral changes could be observed as a function of concentration. It is clear that the spectra of BHmCs in methanol are less concentration-dependent compared to that of the monomeric dye **4**. It is expected that BHmCs in methanol would open up its H-dimeric form (or intermolecular H-aggregates) and give spectral data that are similar to that of **4**. Several factors can influence the spectra of bis-cyanines. The major factors are the magnitude of the interaction between the carbocyanine moieties and the conformational energy of the polymethylene linker. Since the carbocyanine moieties are positively charged, in the intramolecular dimeric complex these dyes most likely have

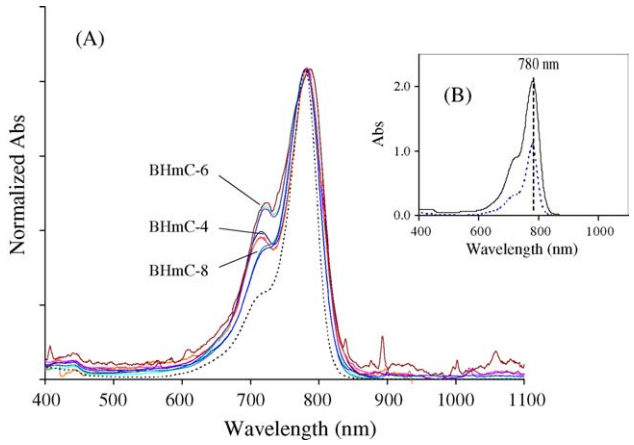

Fig. 2. Absorption spectra of monomeric dye **4** (dotted line) and BHmCs (solid lines) in methanol: (A) concentration effect on the aggregation of BHmCs at three different concentrations, 0.1 μM, 1 μM, and 10 μM. Normalized absorption spectra shown; (B) spectral response comparison (λ_{max} at 780 nm) of **4** and BHmCs at 10 μM.

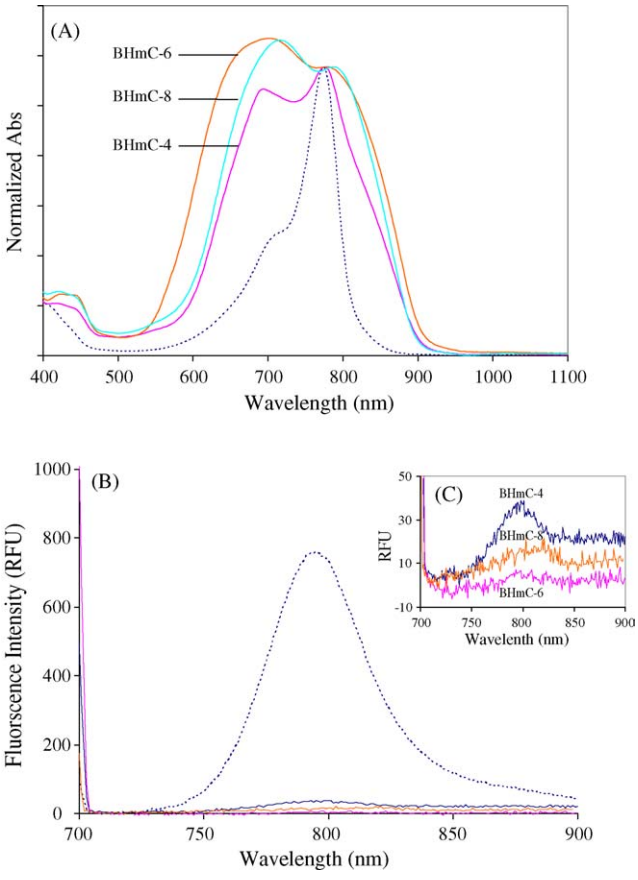

Fig. 3. Spectral comparison of monomeric dye **4** (dotted line) and BHmCs (solid lines) in phosphate buffer, pH 7.2, at 10 μM dye concentration: (A) normalized absorption spectra; (B) and (C) fluorescence emission spectra.

an increased dipole due to charge separation. The two moieties most likely are not in complete overlap, and they are somewhat rotated with respect to one another.

Significant spectral features of BHmC-4 and -6 are observed at around 780 and 720 nm. As judged from absorption at 720 nm, BHmC-6 prefers forming an H-dimer (or H-aggregates). On the other hand, the spectral data for BHmC-4 is consistent with an intermediate state between BHmC-6 and -8. Dye BHmC-8 appears to have a more favorable structure than the others for opening up its clam-shell H-dimer (or to dissociate H-aggregates). To support this hypothesis, the spectral difference between M- and H-bands can be compared. These spectral features indicate an approximately 65 nm difference for both BHmC-4 and -6. Thus, it can be inferred that these dyes exhibit similar properties regarding their H-aggregation. Even at low concentration in methanol, they have similar spectral changes. However it should be noted that the spectral changes at around 720 nm cannot be solely assigned to H-dimerization, since this characteristic band can also be a result of hypsochromic di-, tri-, tetramerization or higher aggregation. Nevertheless, at the low concentrations in methanol this is an unlikely event, owing to the relatively small formation constants of these aggregates [19,20].

Interestingly, BHmC-8 exhibits another particular spectral behavior that is different from those of BHmC-4 and -6. Thus, when the BHmC-8 M-band is compared to those of the other two BHmCs, a slight red shift can be observed as a function of increasing polymethylene chain length. However, BHmC-8 and **4** exhibit a virtually identical lambda maximum at 780 nm, and the molar absorptivity of BHmC-8 is approximately twice as large as that for **4**. This is expected if the two moieties do not interact in methanol (see Fig. 2B). It is reasonable to assume that BHmC-8 in methanol completely opens up from its dimeric form resulting in the aforementioned spectral behavior.

3.1.2. BHmCs in phosphate buffer

Photophysical properties of novel dimeric dyes in 20 mM phosphate buffer at pH 7.2 were characterized. The absorbance spectra of **4** and BHmCs in Fig. 3A were normalized for direct comparison. Significant spectral changes can be observed at around 780 and 700 nm. These spectra in Fig. 3 can be understood by comparing with the spectrum of **4** [14].

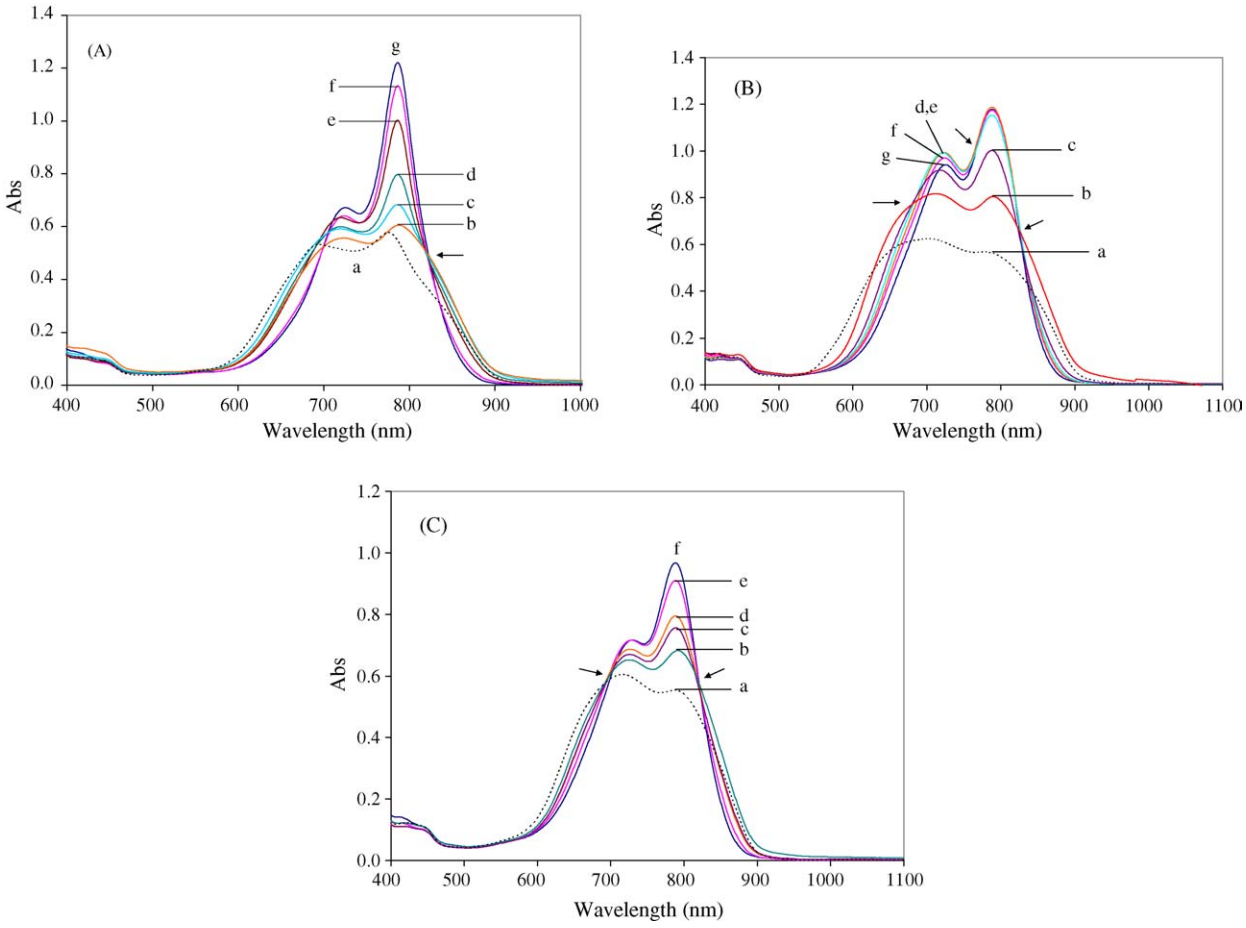

Fig. 4. Absorption of BHmCs (10 μM) in the absence (dotted line) and the presence (solid line) of HSA: (A) BHmC-4 with various HSA concentrations (*a*: 0, *b*: 0.1, *c*: 0.5, *d*: 1, *e*: 5, *f*: 10, *g*: 50 μM); (B) BHmC-6 (*a*: 0, *b*: 1, *c*: 10, *d*: 30, *e*: 50, *f*: 70, *g*: 100 μM); (C) BHmC-8 (*a*: 0, *b*: 1, *c*: 5, *d*: 10, *e*: 50, *f*: 100 μM). The arrows indicate the isosbestic points of BHmCs.

The spectral data of **4** clearly show that it forms intermolecular H-aggregates. It is also clear that BHmCs in Fig. 3B give much lower fluorescence intensity than **4**, indicating strong H-aggregation that can be attributed to intramolecular interaction when compared to **4** [14]. Similar spectral features can be observed for monomeric dyes at much higher concentration [14], so it is plausible to explain that bis(carbocyanines) form intramolecular aggregates. These unique spectral features vary by the length of the polymethylene linker as discussed in Section 3.1.1. In addition, the intramolecular H-aggregates of the dimeric dyes, like the intermolecular H-aggregates of **4,** have negligible fluorescence. This observation is consistent with the well-known dye theories on aggregates [18,19], indicating that dyes forming strong H-aggregates have low fluorescence quantum yield. It is worth noting that the fluorescence of the bis(carbocyanines) is much lower in polar solvents, because they primarily exist in their closed form as opposed to **4** [14,18,19].

It can be seen in Fig. 3A that BHmC-6 forms stronger H-dimer (or intramolecular H-aggregates) compared to the other BHmCs, and the fluorescence intensity of BHmC-6 is the lowest relative to the others. It can be suggested that the hexamethylene bridge in BHmC-6 can attain a low-energy conformation that is favorable for strong intramolecular H-dimerization. According to the spectra shown in Figs. 2 and 3, BHmC-4 exhibits relatively higher monomer and lower H-aggregate bands in the absorption spectra and slightly higher fluorescence intensity than the other BHmCs. On the other hand, BHmC-8 forms a strong intramolecular complex in phosphate buffer.

3.2. BHmC-HSA interaction

3.2.1. Absorption spectra

The absorption spectra of the dimeric dyes in methanol have characteristic bands at 783, 787, and 780 nm for BHmC-4, -6, and -8, respectively. The band intensities are diminished in phosphate buffer. It is likely that these dyes form a strong intramolecular dimer in aqueous solution, but some intermolecular aggregates cannot be ruled out. This spectral shift is most likely the result of the decreased intramolecular π–π^* interactions as the clam-shell opens up. Similar spectral shifts have been observed for the intermolecular aggregates of **4** upon the formation of the dye–HSA complex [14].

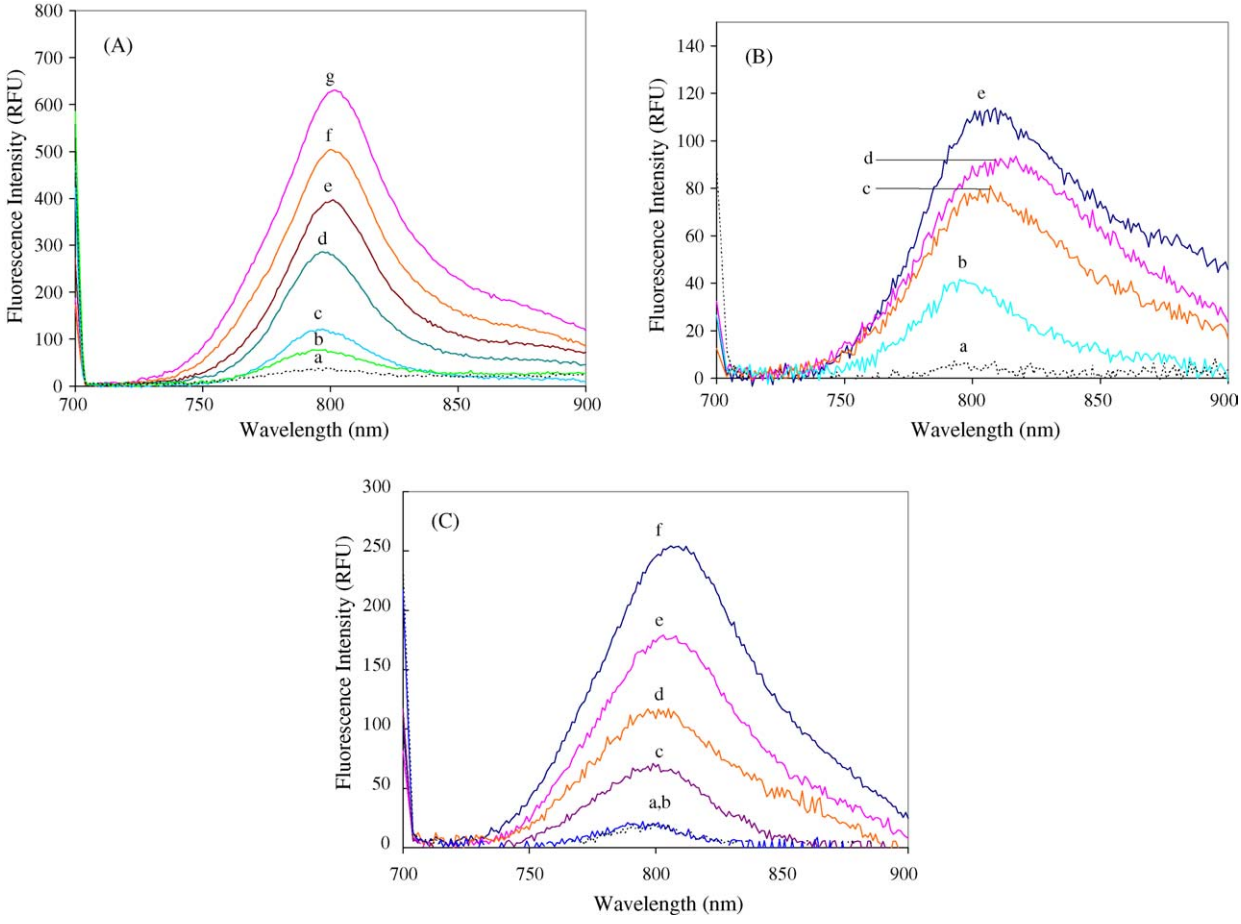

Fig. 5. Fluorescence emission spectra of BHmCs (10 μM) in the absence (dotted line) and the presence (solid line) of HSA: (A) BHmC-4 with various HSA concentrations (*a*: 0, *b*: 0.1, *c*: 0.5, *d*: 1, *e*: 5, *f*: 10, *g*: 50 μM); (B) BHmC-6 (*a*: 0, *b*: 30, *c*: 50, *d*: 70, *e*: 100 μM); (C) BHmC-8 (*a*: 0, *b*: 1, *c*: 5, *d*: 10, *e*: 50, *f*: 100 μM).

Representative absorption spectra of BHmCs in the presence and absence of HSA are given in Fig. 4. Two characteristic bands for individual BHmCs (λ_{max}^{BHC-4} at 776 and 694 nm, λ_{max}^{BHC-6} at 778 and 701 nm, and λ_{max}^{BHC-8} at 788 and 717 nm) can be distinguished in the absorption spectra in buffer solution compared to dye solution in methanol at the same concentration. Upon addition of HSA the inter- and intramolecular aggregates break up with concomitant changes in the H- and M-bands. The absorption spectra of the dimeric dyes at constant concentration of 10 μM with different amounts of HSA added are also depicted in Fig. 4. Upon increase in the HSA concentration, up to 50 μM, and up to 100 μM for BHmC-4, -6, and -8, the characteristic features of the dimeric dye absorption spectra change.

The M-band relative intensity increases significantly in the case of BHmC-4 while the H-aggregate band intensity dramatically decreases. Up to C_{HSA} = 50 μM, a continuous decrease can be observed in the H-band intensity. However, at C_{HSA} = 70 μM, there is negligible change in the intensities of H- and M-bands and absorption of HSA becomes more pronounced. On the other hand, the M-band intensities in BHmC-6 and -8 slightly increase while the H-bands slightly decrease compared to BHmC-4. There are two possibilities for the formation of the BHmC-6 (or -8)–HSA complex. First, these dyes interact with HSA in their open form. The second suggestion is that the intramolecular H-complex and/or intermolecular H-aggregates are bound to the surface or hydrophobic pocket of HSA without opening up the clamshell form. Further studies, similar to those in [21], are needed to determine the actual conformations and biochemical properties of the HSA complex.

In BHmC-6, there is a small spectral change on the M-band compared to BHmC-4. As mentioned above, two binding modes are possible. However, there are three isosbestic points (Fig. 4B) that can be used to estimate the spectral behavior upon interaction with HSA. The first isosbestic point at 677 nm shows that upon the increase in concentration of HSA, H-aggregates are opening up to 30 μM. Consistent with the second isosbestic point (at 767 nm), there seems to be opening up of BHmC-6 at high HSA concentration. During this process, H-dimer (or aggregate) characterized by a band at 721 nm is important since this band decreases in intensity at higher concentrations. It can be inferred that at HSA concentration of more than 50 μM, the HSA expels the H-dimer (or H-aggregates) bound on the surface of HSA. More interestingly, as judged by the bands around 820 nm, all BHmCs show J-aggregation, meaning that these dyes inherently form H-aggregates and J-aggregates and these aggregates are modified upon the addition of HSA.

In BHmC-8, there are two isosbestic points for H- and J-aggregates. According to Fig. 4C, the ratio between M- and H-band is constantly changing without isosbestic point changes upon the increase in HSA concentration. Also, the M-band keeps increasing up to 100 μM HSA. This can be explained by assuming that BHmC-8 predominantly binds to HSA with its open form, as compared to BHmC-6.

Clearly, as HSA concentration increases, the concentration of the inter- and intramolecular H-aggregates free in solution decreases and the fraction of the dimeric dye molecules bound to HSA in its clam-shell form also decreases. This indicates that the interactions of open linear form of BHmC-6 and -8 with HSA are less predominant than the interaction for BHmC-4 because of the presence of intramolecular dimer, even at high HSA concentration. Clearly, binding of BHmC-4 in the open form to HSA is more favorable than those of BHmC-6 and -8.

3.2.2. *Fluorescence spectra*

The fluorescence emission of the dimeric dyes is very weak in aqueous solutions relative to pure methanol. This is very advantageous for utilizing BHmCs as non-covalent labels because the unbound form of the dye to HSA has much lower quantum yield (Fig. 3B). It should be noted that one of the major drawbacks of using **4** and similar monomeric dyes as non-covalent labels is the existence of a relatively strong fluorescence of the unbound free form of the non-covalent label.

The emission spectra of the BHmCs at constant concentration of 10 μM with different amounts of HSA added are given in Fig. 5. Upon an increase in HSA concentration, up

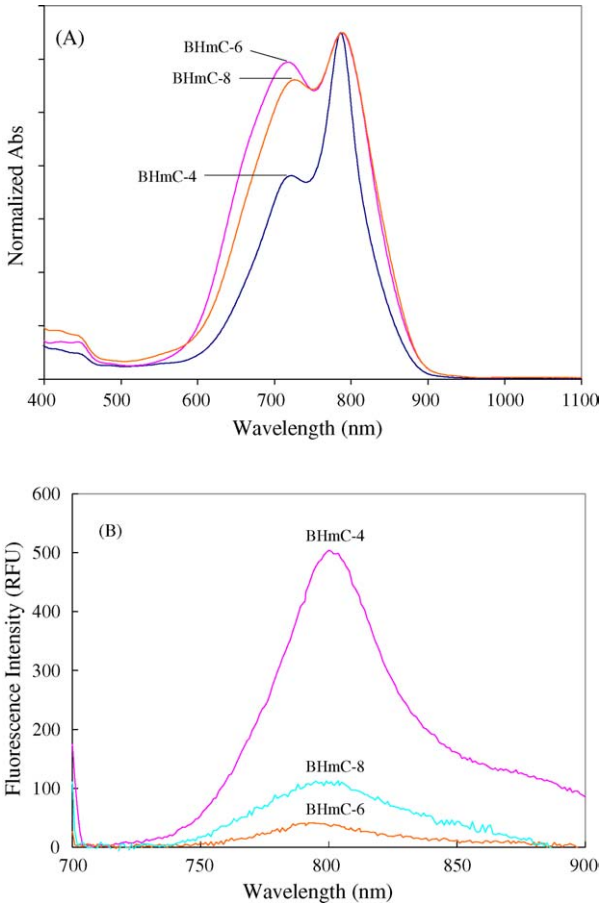

Fig. 6. Spectral comparison of BHmCs (10 μM) regarding their complexes in the presence of HSA (10 μM).

to 50 μM, a strong fluorescence enhancement of BHmC-4 is observed. This can be explained in terms of decreased concentration of weakly fluorescent intra- and intermolecular dye aggregates that are free in solution as the concentration of a highly fluorescent complex of the open linear form of the dye with HSA increases. However, in the spectra of BHmC-6 very small fluorescence changes, even in the presence of HSA, are observed. As can be seen from Fig. 4B, HSA–BHmC-6 complex gives small fluorescence enhancement. While the more rigid intramolecular H-dimer of BHmC-6 partially binds to HSA, BHmC-8 seems to easily open its dimeric form in the presence of HSA, as seen from Fig. 5C. Therefore, one can assume that in its bound form in the presence of HSA, BHmC-8 behaves like an intermediate state between BHmC-4 and -6.

BHmCs and HSA complexes were studied at 10 μM concentrations. Fig. 6A shows that BHmC-6 forms strong intramolecular H-dimer and/or intermolecular H-aggregates which give a high and broad H-band relative to the others. It also shows that upon binding to HSA, BHmC-4 easily opens its intramolecular H-dimer. Importantly, these results indicate that for non-covalent labeling the use of BHmC-4 is more advantageous than the use of the previously published BHmC-10 [14].

4. Conclusions

The spectral work outside the range of autofluorescence of biomolecules is the main advantage of using NIR dyes for labeling of the biomolecules. An additional advantage is gained by using BHmCs as the NIR fluorescent labels. More specifically, the background fluorescence signal produced by monomeric NIR dyes is greatly reduced for BHmCs. The hypsochromic-shifted band (700 nm) of the BHmCs in phosphate buffer indicates their strong inter- and intramolecular interactions. Due to the strong inter- and intramolecular aggregation, the BHmCs show low extinction coefficient and low fluorescence quantum yield. This fluorescence is negligible in the aqueous environment.

BHmCs exhibit diverse interactions with HSA. BHmC-4 easily dissociates its H-aggregates in the presence of HSA. BHmC-6 has a conformationally rigid structure, and its strong intramolecular H-dimer emits low fluorescence. It can be assumed that binding sites of the rigid intramolecular H-dimer of the cationic BHmC-6, in phosphate buffer at pH 7.2, are the hydrophobic cavities and the negatively charged surface of HSA (p*I* 4.8). BHmC-8 exists in a more flexible intramolecular form that can readily open up in methanol while strongly associating into H-aggregates in phosphate buffer.

In summary, these novel bis(heptamethine) cyanine dyes exhibit diverse and favorable characteristics as labels for biomolecules or sensor dyes. Importantly, they seem to be more advantageous than the earlier published BHmC-10. Additional detailed studies are needed to fully develop the analytical utility of these bis-cyanines.

Acknowledgments

We thank Donors of the Petroleum Research Fund, administered by the American Chemical Society, for support of this research.

References

[1] K.B. Male, J.H. Luong, Appl. Biochem. Biotechnol. 61 (1996) 267.
[2] C.Q. Zhu, H. Zheng, D.H. Li, S.H. Li, J.G. Xu, Chin. J. Chem. 22 (2004) 1319.
[3] L. Tarazi, N. Narayanan, G. Patonay, Microchem. J. 64 (2000) 247.
[4] M.I. Daneshvar, J.M. Peralta, G.A. Casay, N. Narayanan, L. Evans, G. Patonay, L. Strekowski, J. Immunol. Methods 226 (1999) 119.
[5] J. Sowell, J.C. Mason, L. Strekowski, G. Patonay, Electrophoresis 22 (2001) 2512.
[6] E. Waddell, Y. Wang, W. Stryjewski, S. McWhorter, A.C. Henry, D. Evans, R.L. McCarley, S.A. Soper, Anal. Chem. 72 (2000) 5907.
[7] M.B. Baars, G. Patonay, Anal. Chem. 71 (1999) 667.
[8] B.L. Legendre Jr., D.L. Moberg, D.C. Williams, S.A. Soper, J. Chromatogr. A 779 (1997) 185.
[9] G. Patonay, M.D. Antoine, A.E. Boyer, Proc. SPIE 1435 (1991) 52.
[10] E.E. Jelley, Nature 138 (1936) 1009.
[11] E.E. Jelley, Nature 139 (1937) 631.
[12] W.J. Harrison, D.L. Mateer, G.J. Tiddy, J. Phys. Chem. 100 (1996) 2310.
[13] V. Czikkely, H.D. Forsterling, H. Kuhn, Chem. Phys. Lett. 6 (1970) 207.
[14] G. Patonay, J.S. Kim, R. Kodagahally, L. Strekowski, Appl. Spectrosc., in press.
[15] A.H. Herz, Adv. Colloid Interface Sci. 8 (1977) 237.
[16] F.A. Schaberle, V.A. Kuz'min, I.E. Borissevitch, Biochim. Biophys. Acta 1621 (2003) 183.
[17] J. Xiang, X. Yang, C. Chen, Y. Tang, W. Yan, G. Xu, J. Colloid Interface Sci. 258 (2003) 198.
[18] S.M. Makin, L.I. Boiko, O.A. Shavrygina, Zh. Org. Khim. 13 (1977) 1189.
[19] D.M. Sturmer, D.W. Heseltine, in: T.H. James (Ed.), The Theory of the Photographic Process, fourth ed., 1977.
[20] H. Zollinger, Color Chemistry, VCH Publishers, 1991.
[21] P. Theodore, All about Albumin, Academic Press, 1996.